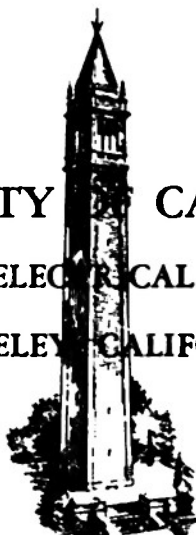


AD No. / 8941

ASTIA FILE COPY

UNIVERSITY OF CALIFORNIA
DIVISION OF ELECTRICAL ENGINEERING
BERKELEY, CALIFORNIA



ELECTRONICS RESEARCH LABORATORY
ANTENNA GROUP

OBSTACLES AND DISCONTINUITIES
IN A MULTIMODE WAVEGUIDE

by
Gedaliah Held
and
Wolfgang Kummer

Institute of Engineering Research
Technical Report

Series No. 60, Issue No. 101

August 1, 1953

DIVISION OF ELECTRICAL ENGINEERING
ELECTRONICS RESEARCH LABORATORY

Series No. 60
Issue No. 101

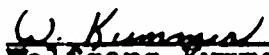
ANTENNA GROUP

Report No. 20 on
Office of Naval Research
Contract N7onr-29529

OBSTACLES AND DISCONTINUITIES IN A MULTIMODE
WAVEGUIDE

Prepared by:


Gedaliah Held, Graduate Research Engineer


Wolfgang Kummer, Graduate Research Engineer

Edited by:


Samuel Silver, Professor of Engineering Science

Approved by:


J.R. Whinnery, Vice-Chairman, Division of Electrical
Engineering, in charge of Electronics Research
Laboratory

ABSTRACT

General considerations are developed concerning equivalent circuit representations of obstacles and discontinuities of a general type in waveguides which support free propagation of several modes. It is shown that the scattering matrix is symmetrical in the general case including dissipative types of discontinuities in structures such as slots in the wall. This means that the network representation is valid in multimode waveguide.

Special application is made to the case of a half-wave rectangular slot in the wall of a rectangular waveguide propagating the TE_{10} and TE_{20} modes. The symmetry of the scattering coefficients is in good agreement with that predicted theoretically on the assumption that the distribution of the excitation (though not the level) is determined by the slot and not by the exciting mode. This assumption is substantiated also by observed radiation patterns.

INTRODUCTION

A considerable amount of work has been done establishing the representation of an obstacle by an equivalent circuit and the transmission line analogy of a waveguide propagating one mode. Multimode waveguides are becoming of importance in practical applications and there is a need, therefore, for an extension of equivalent circuit analysis to the multimode system. This paper is a report on the initial phases of studies which we are making in this field. The basis for equivalent circuit representation is established and application is made to the problem of a slot. Measurements techniques and the fundamental considerations which must be applied to the correct interpretation of the data are reviewed.

If we are to look upon the waveguide as a set of transmission lines, we must be able to represent the discontinuity by an impedance matrix (Z), where (Z) relates the equivalent voltage and current matrices through Ohm's law $(V)=(Z)(I)$. Since the system is bilateral, linear, and isotropic, the matrix (Z) will be symmetrical in the sense that $Z_{ik}=Z_{ki}$. If (S) is a scattering matrix such that $(B) = (S)(A)$ where (A) and (B) are the column matrices of the incident and reflected waves respectively, then the impedance matrix is given by⁽¹⁾

$$(Z) = [(I)-(S)]^{-1} [(I) + (S)] \quad (1)$$

It is readily shown that if $S_{ik} = S_{ki}$, $Z_{ik} = Z_{ki}$; and conversely. We see now that it is sufficient to investigate the symmetry

properties of the scattering matrix, (S).

WAVEGUIDE MODES

Consider a waveguide with an obstacle in it. In the region far from the obstacle the fields will be (2) for TE modes

$$\begin{aligned}\underline{H} &= e^{-\gamma z} \left(-\frac{\gamma}{\kappa^2} \nabla u + u \underline{i}_z \right) \\ \underline{E} &= \frac{\omega \mu}{j\gamma} (\underline{H} \times \underline{i}_z)\end{aligned}\quad (2)$$

and for TM modes

$$\begin{aligned}\underline{H} &= \frac{\omega \epsilon}{j\gamma} (\underline{E} \times \underline{i}_z) \\ \underline{E} &= e^{-\gamma z} \left(-\frac{\gamma}{\kappa^2} \nabla v + v \underline{i}_z \right)\end{aligned}\quad (3)$$

$$\text{where } \gamma_{mn} = j\beta_{mn} = (\kappa_{mn}^2 - k^2)^{\frac{1}{2}} \quad (4)$$

and $u = u(x, y)$ and $v = v(x, y)$

The power flow P we equate to unity

$$P = 1/2 \int_{\sigma} \text{Re}(\underline{E} \times \underline{H}) \cdot \underline{n} \, d\sigma = 1 \quad (5)$$

and if we normalize the eigen function u and v so that

$$\int_{\sigma} (\Delta u)^2 \, d\sigma = 1 \text{ and } \int_{\sigma} (\Delta v)^2 \, d\sigma = 1 \quad \text{then} \quad (6)$$

for all modes we get the normalization factors

$$\begin{aligned}a &= \sqrt{\frac{2}{\mu\beta\omega}} |\kappa|^2 \quad \text{for } u = u(x, y) \\ a &= \sqrt{\frac{2}{\epsilon\beta\omega}} |\kappa|^2 \quad \text{for } v = v(x, y)\end{aligned}\quad (7)$$

Let us denote now waves propagating to the right and left with a (-) and (+) index respectively

$$\begin{array}{ll} \text{to right} & \text{to left} \\ \underline{E}_1^- = \psi_1^-(x, y) e^{-\gamma z} = e_1^- & \underline{E}_1^+ = \psi_1^+(x, y) e^{+\gamma z} = e_1^+ \\ \underline{H}_1^- = \psi_1^-(x, y) e^{-\gamma z} = h_1^- & \underline{H}_1^+ = \psi_1^+(x, y) e^{+\gamma z} = h_1^+ \end{array} \quad (8)$$

Every field in the waveguide will then be a linear combination of the eigen vectors, e_i and h_i , that represent modes.

Suppose now we designate by $S_{ki}^{12} a_i^1$ the amplitude of the k th mode in region 2 due to the i th mode of amplitude a_i^1 striking the obstacle in region 1. Then if a wave of mode 1 will strike the obstacle in both regions (1) and (2) with amplitudes a_i^1 and a_i^2 respectively, the fields due to it will be

$$\begin{aligned} E_1^1 &= a_i^1 e_i^- + \sum_{k=1}^{\infty} S_{ki}^{11} a_i^1 e_k^+ + \sum_{k=1}^{\infty} S_{ki}^{21} a_i^2 e_k^+ \quad \text{for } z < 0 \\ E_1^2 &= a_i^2 e_i^+ + \sum_{k=1}^{\infty} S_{ki}^{12} a_i^1 e_k^- + \sum_{k=1}^{\infty} S_{ki}^{22} a_i^2 e_k^- \quad \text{for } z > 0 \end{aligned} \quad (9)$$

and similar expressions for H except that h_i stands for e_i .

In general if we have several modes incident we add all these fields together. Since we can also write

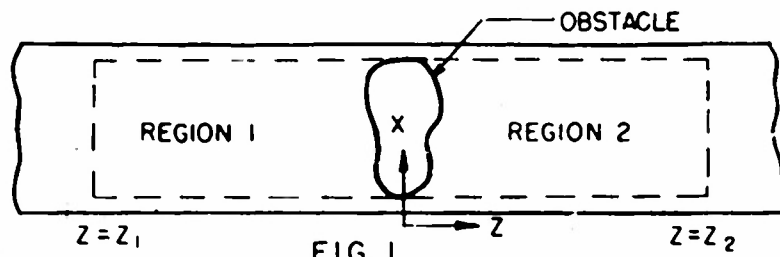
$$\begin{aligned} E^1 &= \sum_{i=1}^{\infty} a_i^1 e_i^- + b_i^1 e_i^+ \quad z < 0 \\ E^2 &= \sum_{i=1}^{\infty} a_i^2 e_i^+ + b_i^2 e_i^- \quad z > 0 \end{aligned} \quad (10)$$

We get, upon writing out the expressions explicitly,

$$\begin{aligned} b_k^1 &= \sum_i S_{ki}^{11} a_i^1 + S_{ki}^{21} a_i^2 \\ b_k^2 &= \sum_i S_{ki}^{12} a_i^1 + S_{ki}^{22} a_i^2 \end{aligned} \quad (11)$$

Upon changing order of numeration, so that index 2 on top starts after N on bottom, where N is number of propagating modes, we get $(B) = (S)(A)$ where (S) is the scattering matrix defined before. We investigate now the properties of the elements S_{ik} of this matrix.

SCATTERING MATRIX OF A DISCONTINUITY



To investigate the properties of S_{1k} we consider a region that includes the obstacle and is bounded by the inner walls, and two cross sections at $z=z_1 < 0$ and $z=z_2 > 0$. Since we consider a source free region the divergence of the field vectors is zero, and to two fields $E^{(m)}, H^{(m)}$, and $E^{(n)}, H^{(n)}$ of the same frequency, that satisfy Maxwell's equations, we can apply the Lorentz theorem:

$$\int_V (\mathbf{E}^{(m)} \times \mathbf{H}^{(n)} - \mathbf{E}^{(n)} \times \mathbf{H}^{(m)}) \cdot \bar{n} d\sigma = 0 \quad (12)$$

In this region we apply the theorem to two fields due to particular modes set up in particular ways to give the desired relationships between the elements of the scattering matrix (S).

If we consider first the field due to mode 'm' of unit amplitude incident from left and mode 'n' of unit amplitude incident from right, and express these fields by expressions similar to (9), then substituting in (12), making use of the normalization and orthogonality of the eigen vectors e_v and h_v , we get

$$2(s_{mm}^{21} - s_{mm}^{12}) + \int_{\sigma \text{ walls}} (\mathbf{E}^{(m)} \times \mathbf{H}^{(n)} - \mathbf{E}^{(n)} \times \mathbf{H}^{(m)}) \cdot \bar{n} d\sigma = 0 \quad (13)$$

We consider now three general cases.

Case a - Lossless obstacles (perfectly conducting) in a closed waveguide. In this case the boundary conditions on $E^{(m)}, H^{(m)}$ and $E^{(n)}, H^{(n)}$

$$\begin{aligned}\bar{n} \times \bar{E} &= 0 \\ \bar{n} \cdot \bar{H} &= 0\end{aligned}\tag{14}$$

tell us immediately that the integral in (13) vanishes.

Case b -Lossy obstacles (dielectrics, etc.) in a closed waveguide. In this case we change our volume and surface of integration. The integrals over the perfectly conducting part of the wall vanish as in case a, and we are left with an integral over the outer surface of the obstacle. We apply the same theorem to the volume of the obstacle. The surface of integration is now the inner walls of the obstacle. We have then

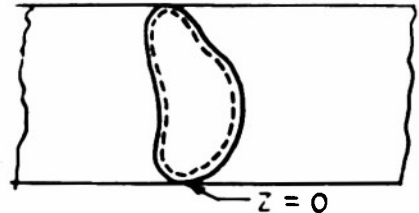


FIG. 2

$$\int_{\text{inner surface}} (\bar{E}^{(n)} \times \bar{H}^{(m)} - \bar{E}^{(m)} \times \bar{H}^{(n)}) \cdot \bar{n} d\sigma = \int \bar{F} \cdot \bar{n} d\sigma = 0\tag{15}$$

and the integral over the inner surface vanishes. Now, since in expression (15) only the tangential components of E and H contribute, and by the boundary conditions we know that the tangential components go over continuously across the boundary, we have

$$F \text{ inside} = F \text{ outside}\tag{16}$$

and therefore in this case, too, we are left with

$$S_{mn}^{21} - S_{nm}^{12} = 0\tag{17}$$

Case c -Radiating obstacles-slots in waveguide wall. In this case, applying the theorem, we will be left with an integral over the inner boundary of the slot.

$$\int_{\text{slot}} \bar{H}_n \cdot \bar{n} d\sigma\tag{18}$$

We use now a similar technique to the one used in case b. We apply the Lorentz theorem to the outside region.

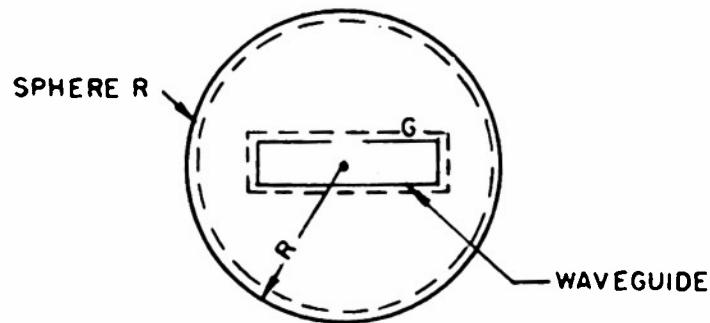


FIG. 3

We have now

$$\int_{\text{sphere } R} \bar{F} \cdot \bar{n} \, d\sigma + \int_{\text{slot out}} F \cdot \bar{n} \, d\sigma + \int_{\text{over } G} \bar{F} \cdot \bar{n} \, d\sigma = 0 \quad (19)$$

As in case a, over G the integral goes to zero due to conditions (14). We consider now the case where the radius of the sphere R goes to infinity.

$$\int_{\sigma} \bar{F} \cdot \bar{n} \, d\sigma = \lim_{R \rightarrow \infty} \int R \cdot \bar{F} \, dR \quad (20)$$

and as F is a combination of the radiation fields due to the respective modes, it will satisfy the Sommerfeld radiation conditions. We get then

$$\int_{\sigma_{\text{out}}} \bar{F} \cdot \bar{n} \, d\sigma = 0$$

and consequently

$$\int_{\text{slot}} \bar{F}_{\text{out}} \cdot \bar{n} \, d\sigma = 0 \quad (21)$$

By the same argument about the continuity of the tangential component as in case b, we see that

$$\int_{\text{slot}} \bar{F}_{\text{in}} \cdot \bar{n} \, d\sigma = \int_{\text{slot}} \bar{F}_{\text{out}} \cdot \bar{n} \, d\sigma = 0 \quad (22)$$

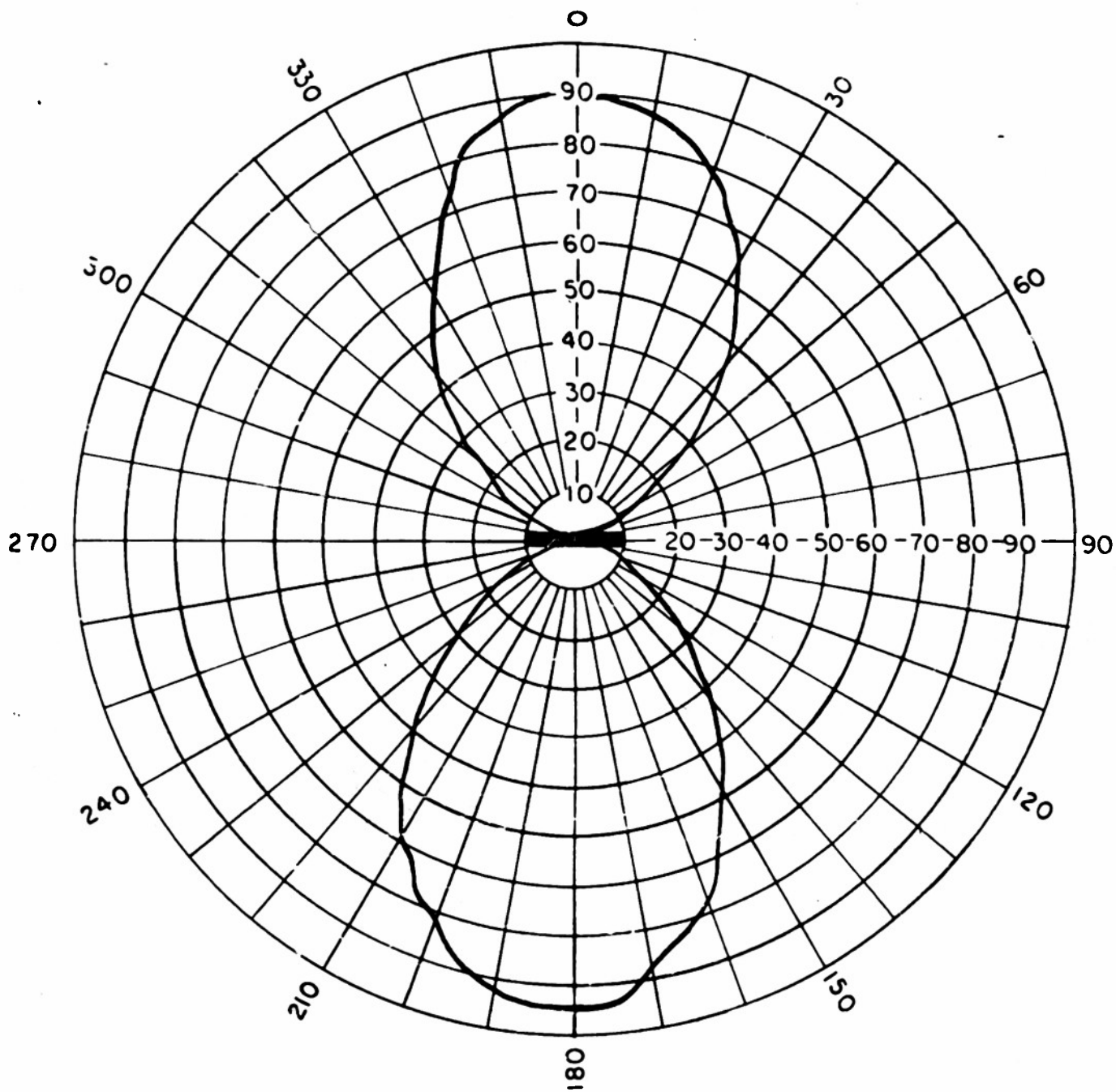
and in this way we conclude the symmetry of the respective elements of (S) for any general obstacle.

Applying the same argument to the field due to mode m and n both incident from either left or right we get the required relation for all the necessary elements.

This establishes the validity of representing a multimode waveguide with discontinuities as a system of transmission lines with certain coupling networks between the lines. The general theory thus becomes one of multipole networks made up of distributed constant elements.

One of the class of obstacles of importance in multimode waveguides are slots cut in the walls of the guides. In multimode guide the slot can be characterized by a scattering matrix whose coefficients can be determined experimentally. Slot arrays can be analyzed by combining either the scattering matrices or the impedance matrices of the individual elements. In the analysis to follow we will confine ourselves to the half-wave narrow slot. On the assumption that the slot excitation does not change in shape with the exciting mode, it is possible to calculate the reflection and transmission coefficients of the slot. This assumption is justified by the fact that the radiation patterns are sensibly independent of the exciting mode. Fig. 4 shows a sample of the patterns which were all of identical shape, only changing in envelope amplitude due to the different slot couplings.

For a given excitation $E_0 \cos ks$ in the slot, the amplitude of the TE_{m0} mode generated by the longitudinal slot cut in the broad face of the guide is



POWER MEASUREMENTS MADE OF
 TE_{20} SIGNAL, VERTICAL
 POLARIZATION, H-PLANE

FIG. 4. HORIZONTAL RADIATION PATTERN
 FOR 0.630" x 0.015" SLOT

$$A_{m0} = -\frac{\sqrt{2}}{4} \frac{\omega E_0 \left(\frac{k}{k_{m0}}\right) \lambda_{g0}}{\pi^2} \frac{V_{m0}}{|V_{m0}|} \cos \frac{m\pi x}{a} \cos \frac{\beta_{m0} \lambda}{4} \quad (23)$$

where

A_{m0} = voltage amplitude of the m^{th} mode

ω = width of slot

E_0 = peak field intensity in slot

$k = \frac{2\pi}{\lambda}$, $k_{m0}^2 = m^2 \frac{b}{a}$, b = height of guide, a = width of guide

V = rms voltage across guide

x = distance across broad face of guide measured from edge

λ , λ_{g0} = free space and guide wavelengths

$$\beta_{m0} = \frac{2\pi}{\lambda_{g0}}$$

Hence the ratio of the coefficients for the TE_{20} and TE_{10} modes, corresponding to a given E_0 generated by the incident wave is*

$$\frac{A_{20}}{A_{10}} = \frac{1}{2} \left(\frac{\lambda_{g20}}{\lambda_{g10}} \right)^{\frac{1}{2}} \frac{\cos \frac{\beta_{20} \lambda}{4} \cos \frac{2\pi x}{a}}{\cos \frac{\beta_{10} \lambda}{4} \cos \frac{\pi x}{a}} \quad (24)$$

As noted above the slot voltage is eliminated in this expression. The equation becomes indeterminate for positions $1/4$, $1/2$, and $3/4$ of the guide width. At these points one or the other of the modes does not couple to the slot and hence there are no scattered waves for the particular mode. Due to

*The normalization differs from that in reference 3. We normalize each mode so that unity power flows down for each mode.

the physical symmetry of the slot, the reflection and transmission amplitudes will be equal for the same mode.

Fig. 5 and Fig. 6 show that while the amplitudes are not the same for the different mode excitations the ratio of A_{20} to A_{10} remains constant. Experiment shows this ratio to be approximately 9 db. while (24) gives 10.6 db.

The conclusions derived theoretically have been checked experimentally using half-wave narrow slots cut in the wall of rectangular waveguide propagating TE_{10} and TE_{20} modes.

The measurement techniques used are applicable to any obstacle problems in multimode guide. The apparatus, described in detail previously⁽¹⁾, consists of two-mode transducers, two-mode standing wave detector, and a null detector system made up of a phase shifter, precision attenuator, and magic tee. The two-mode transducer makes it possible to mix and separate each of the modes in the two mode guide; the two-mode standing wave detector directly measures the VSWR of each mode in the presence of the other. Referring to Fig. 7 we see that if we send down TE_{10} in the standard guide, TE_{20} will be propagated in the two-mode guide. For the slot in a general position both TE_{10} and TE_{20} modes will be transmitted and reflected by it. These scattered waves will all be absorbed by matched loads. The TE_{20} reflected toward the incident signal is measured by a standing wave detector in the single mode guide through the matched two-mode exciter. It is of course possible to insert the two-mode standing wave detector and obtain the same result. The TE_{10} wave can also be measured, giving, however,

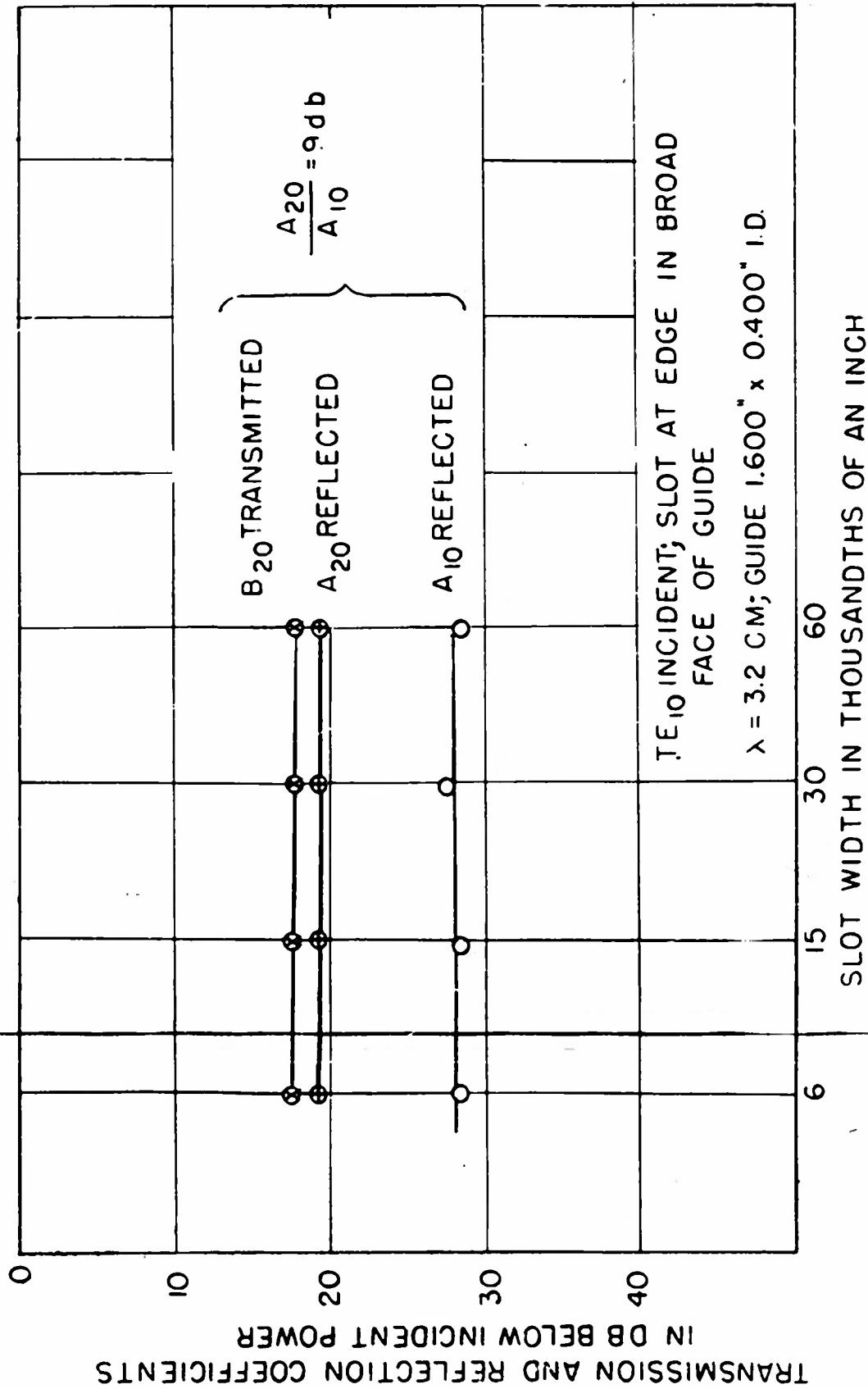


FIG. 5 TRANSMISSION AND REFLECTION COEFFICIENTS FOR 1/2 WAVELENGTH LONGITUDINAL SLOT AS A FUNCTION OF SLOT WIDTH.

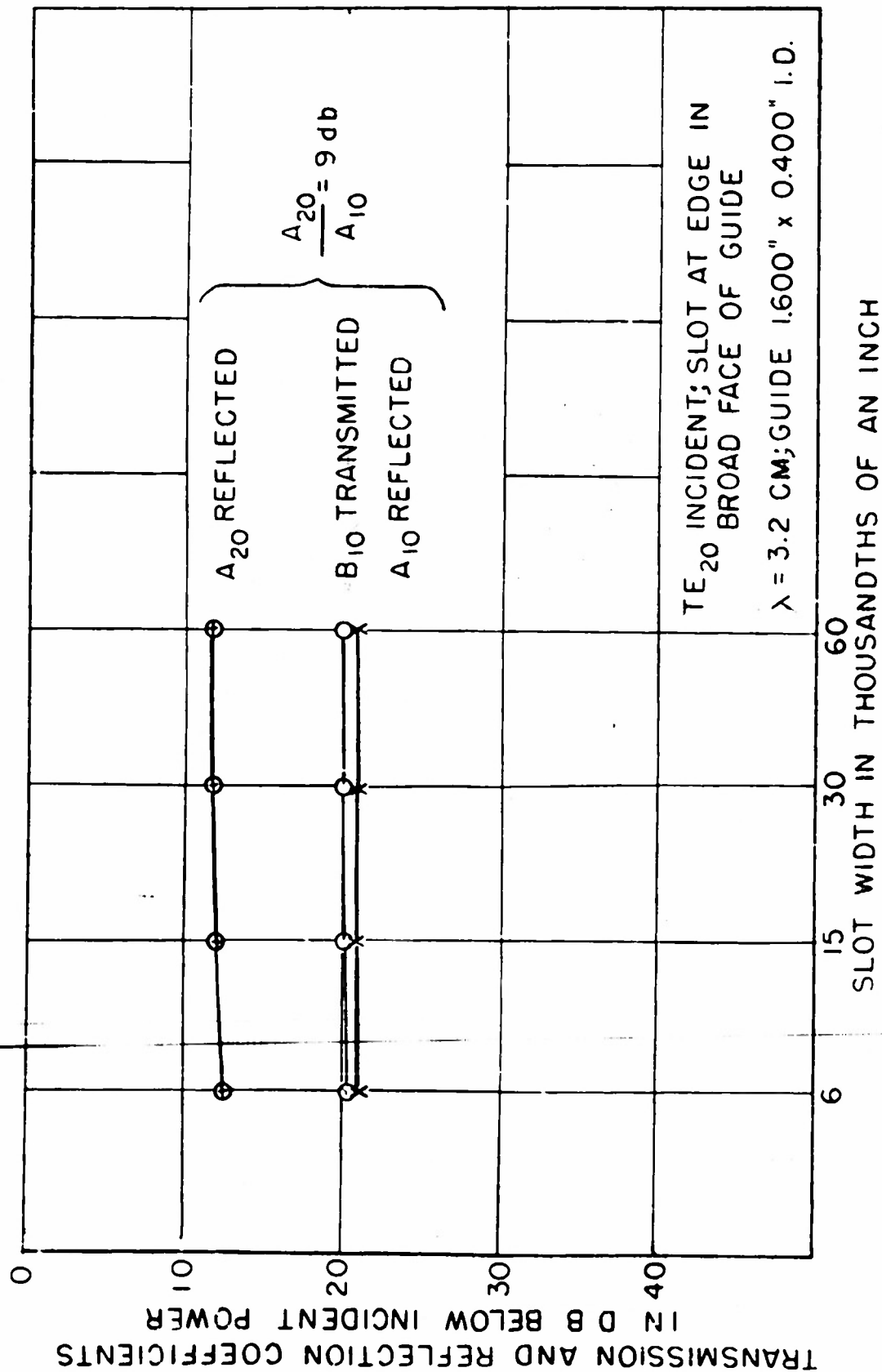


FIG.6 TRANSMISSION AND REFLECTION COEFFICIENTS FOR 1/2 WAVELENGTH LONGITUDINAL SLOT AS A FUNCTION OF SLOT WIDTH.

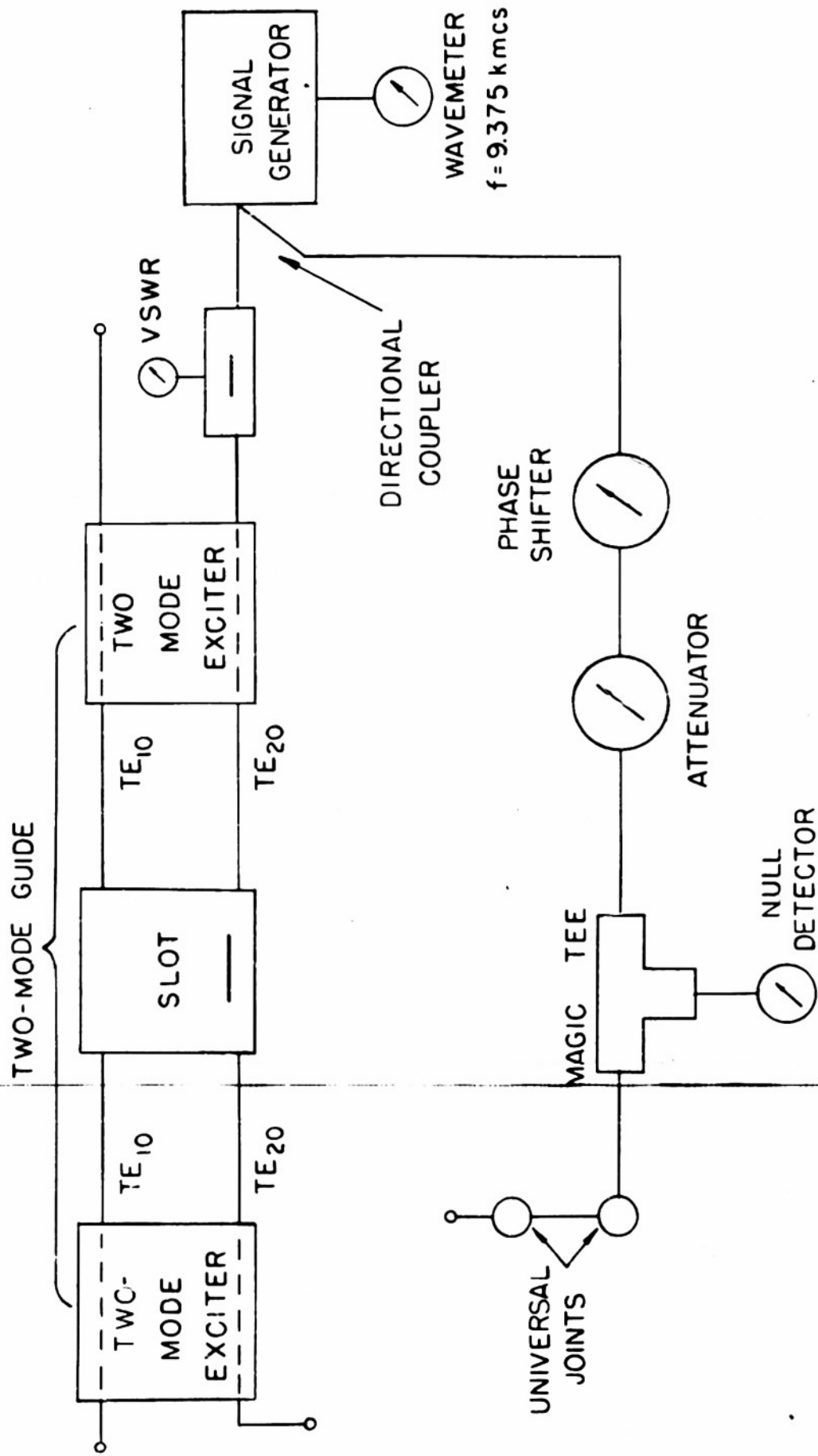


FIG 7 SCHEMATIC LAYOUT FOR MEASURING TRANSMISSION AND REFLECTION COEFFICIENTS WITH TE_{20} INCIDENT ON SLOT

only its amplitude because all modes are terminated in matched loads. The other scattered components are measured by comparing each one of them with a reference signal coming from the directional coupler.

Similarly the system can be connected for TE_{10} incident on the slot.

We can show that the elements of the scattering matrix seen in the arms of a matched transducer are the same as those we would see in the multimode

guide. Let us consider the v th arm of the transducer as an obstacle with a scattering matrix g_v . This is shown

schematically in the diagram.

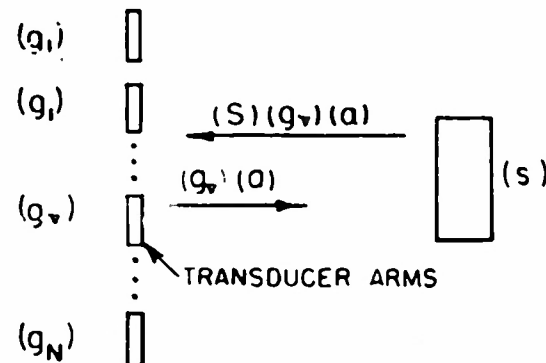


FIG. 8

A wave of amplitude (a) in arm v will not be reflected due to matching, and in the multimode region will be $(a)(g_v)$. At the obstacle it undergoes reflection, and a wave $(a)(g_v)(S)$ will strike arm μ . Due to matching again there is no reflection, and in arm μ we see a wave of amplitude

$$b' = (a)(g_v)(S)(g_\mu)$$

So the effective scattering matrix as seen is

$$S' = (g_v)(S)(g_\mu)$$

For the matched case the matrices g_v will satisfy the conditions

$$(g_v)(g_\mu) = 0 \text{ where } v \neq \mu$$

and $(g_v)(g_v) = I$ where I is the unit matrix.

In our experimental set-up we have only two modes, so,

due to matching we have

$$g_1 = \begin{pmatrix} 0 & 0 & 1 & 0 \\ 0 & 0 & 0 & 0 \\ 1 & 0 & 0 & 0 \\ 0 & 0 & 0 & 0 \end{pmatrix} \quad \text{and} \quad g_2 = \begin{pmatrix} 0 & 0 & 0 & 0 \\ 0 & 0 & 0 & 1 \\ 0 & 0 & 0 & 0 \\ 0 & 1 & 0 & 0 \end{pmatrix}$$

and, for example, in arm two we will see the following:

$$S' = (g_1)(S)(g_2) \begin{pmatrix} 0 & 0 & 1 & 0 \\ 0 & 0 & 0 & 0 \\ 1 & 0 & 0 & 0 \\ 0 & 0 & 0 & 0 \end{pmatrix} \begin{pmatrix} s_{11}^{11} & s_{12}^{11} & s_{11}^{12} & s_{12}^{12} \\ s_{11}^{11} & s_{12}^{11} & s_{11}^{12} & s_{12}^{12} \\ s_{21}^{11} & s_{22}^{11} & s_{21}^{12} & s_{22}^{12} \\ s_{21}^{11} & s_{22}^{11} & s_{21}^{12} & s_{22}^{12} \\ s_{11}^{21} & s_{12}^{21} & s_{11}^{22} & s_{12}^{22} \\ s_{11}^{21} & s_{12}^{21} & s_{11}^{22} & s_{12}^{22} \\ s_{21}^{21} & s_{22}^{21} & s_{21}^{22} & s_{22}^{22} \\ s_{21}^{21} & s_{22}^{21} & s_{21}^{22} & s_{22}^{22} \end{pmatrix} \begin{pmatrix} 0 & 0 & 0 & 0 \\ 0 & 0 & 0 & 1 \\ 0 & 0 & 0 & 0 \\ 0 & 1 & 0 & 0 \end{pmatrix}$$

$$= \begin{pmatrix} 0 & s_{12}^{22} & 0 & s_{12}^{21} \\ 0 & 0 & 0 & 0 \\ 0 & s_{12}^{12} & 0 & s_{12}^{11} \\ 0 & 0 & 0 & 0 \end{pmatrix}$$

This shows that the scattering coefficients are not altered when measured in the single mode guide, provided, of course, that the transducers do not cross-couple modes, and are matched.

REFERENCES

1. Montgomery, Dicke and Purcell, Principles of Microwave Circuits, Vol. 8 MIT Series, McGraw-Hill, 1948. pp. 146-148.
2. S. Silver, Microwave Antenna Theory and Design, Vol. 12, MIT Series, McGraw-Hill, 1949, pp. 205-207.
3. S. Silver, Microwave Antenna Theory and Design, Vol. 12, MIT Series, McGraw-Hill Co., 1949, pp. 287-295.
4. W. Kummer, "Impedance Measurement Techniques for Two-Mode Guides" Trans. of the IRE, PGAP-1, Feb. 1952, pp. 148-152.

Distribution:

Chief of Naval Research, Washington, D.C. (Code 427)	2
Naval Research Laboratory, (Code 2000)	9
Chief of Naval Research, (Code 460)	1
Naval Research Laboratory (Code 2020)	2
Naval Research Laboratory (Code 3480)	1
BuShips (Code 838D)	1
BuShips (Code 810)	1
Bureau of Ordnance (Relf)	1
Bureau of Ordnance (AD3)	1
Bureau of Aeronautics (EL51)	1
Bureau of Aeronautics (EL1)	1
Chief of Naval Operations (Op-413)	1
Chief of Naval Operations (Op-20)	1
Chief of Naval Operations (Op-32)	1
Naval Air Development Station, Electronics Laboratory	1
O.N.R., New York	1
O.N.R., San Francisco	2
O.N.R., Boston, Massachusetts	1
O.N.R., Chicago, Illinois	1
O.N.R., Pasadena, California	1
Assistant Naval Attache for Research	2
Naval Ordnance Laboratory	1
U.S.N.E.L., San Diego, California	2
U.S. Naval Academy, Electrical Eng. Dept., Annapolis	1
Commandant Coast Guard (EKE)	1
Office of the Chief Signal Officer (SIGET)	1
Signal Corps Engineering Laboratories, Attn: Mr. Woodyard	1
Electronics Laboratory, Wright Field (MCREKR)	1
AMC Watson Laboratories, Attn: Dr. P. Newman	1
AMC Cambridge Research Laboratory, Attn: Dr. Spencer	1
Headquarters, U.S. Air Force (AEMEN-2)	1
Research and Development Board, Washington, D.C.	1
National Bureau of Standards	1
Cruft Laboratory, Harvard University, Attn: Prof. King	1
Mass. Institute of Technology, Attn: Prof. L.J. Chu	1
Stanford University, Attn: Dean F.E. Terman	1
E.E. Department, Illinois University, Attn: Prof. Jordan	1
Ohio State University Research Foundation, Dr. Rumsey	1
E.E. Department, Cornell University, Attn: Dr. H.G. Booker	1
Stanford Research Institute, Attn: Dr. J.V.N. Granger	1
Polytechnic Institute of Brooklyn, Attn: Dr. A. Oliner	1
Washington Square College, N.Y.U. Math Group, Attn: Prof Kline	1
Squier Signal Laboratory, Attn: Vincent J. Kublin	1
Flight Determination Laboratory, Attn: M.A. Krivanich	1
Department of Commerce	1
Armed Services Technical Information Agency	5